INTERNATIONAL JOURNAL FOR NUMERICAL METHODS IN FLUIDS
Int. J. Numer. Meth. Fluids **31**: 879–889 (1999)

UPWIND SCHEMES AND LARGE EDDY SIMULATION

T.K. SENGUPTA* AND MANOJ T. NAIR

Department of Aerospace Engineering, Indian Institute of Technology, Kanpur 208 016, India

SUMMARY

Upwind schemes are evaluated with respect to their spectral accuracy in solving advection–diffusion equations. Their connection to large eddy simulations (LES) and direct numerical simulations is explored. Some broad guidelines are set forth to select an appropriate scheme for simulating a Navier–Stokes equation with or without a subgrid-scale model. Copyright © 1999 John Wiley & Sons, Ltd.

KEY WORDS: upwind schemes; large eddy simulation; direct numerical simulation

1. INTRODUCTION

The use of higher-order upwind schemes to solve the Navier–Stokes equation has seen an upsurge in recent times following the early success of Kawamura *et al.* in predicting the drag crisis faced by a circular cylinder in the critical Reynolds number range [1]. Similar successes have also been noted by the present authors in simulating high-Reynolds number flows past various two-dimensional bodies in Sengupta and Sengupta [2], Nair and Sengupta [3] and Sengupta and Nair ['Unsteady flows past two-dimensional lifting bodies' (under review for *Int. J. Numer. Methods Fluids*, 1999)].

Various interpretations have been forwarded over the years to explain the success of this particular scheme and other higher-order upwind schemes. In this work, we have attempted to generalize the explanations given earlier in Sengupta and Sengupta [2]. In view of this, we also discuss the various compact different schemes that have been proposed by Lele [4] and the various filters that are used in large eddy simulations (LES) and discussed in Spyropoulos and Blaisdell [5].

In Sengupta and Sengupta [2] and Schumann [6] it was mentioned that discretizing the continuum Navier–Stokes equation is equivalent to introducing an appropriate low-pass filter. It is now well known that the success of high-Reynolds number flow simulations rests predominantly on the way the convection terms are discretized. These are done according to

$$\left(f\frac{\partial u}{\partial x}\right)_i = f_i\frac{-u_{i+2}+8(u_{i+1}-u_{i-1})+u_{i-2}}{12\Delta x}+|f_i|\frac{u_{i+2}-4u_{i+1}+6u_i-4u_{i-1}+u_{i-2}}{4\Delta x} \tag{1}$$

for the third-order upwinding schemes used in Kawamura *et al.* [1] and Sengupta and Sengupta [2].

Now, if we represent the unknown by its spectral representation

* Correspondence to: Convenor, CFD Laboratory, Department of Aerospace Engineering, Indian Institute of Technology, Kanpur 208 016, India.

CCC 0271–2091/99/210879–11$17.50

Received November 1997
Revised July 1998

$$u(x) = \frac{1}{2\pi} \int_{-\infty}^{\infty} \hat{u}(k) \exp(-ikx)\, \mathrm{d}k, \tag{2}$$

then the exact spectral representation of the derivative is given by

$$\frac{\mathrm{d}u}{\mathrm{d}x} = \int_{-\infty}^{\infty} -\imath k \hat{u}(k) \exp(-\imath kx)\, \mathrm{d}k. \tag{3}$$

When we represent the same derivative by finite differences—as we have shown in Equation (1)—the discrete derivative can be written as

$$\frac{\mathrm{d}u}{\mathrm{d}x} = \int_{-k_{\max}}^{k_{\max}} -\imath k_{\mathrm{eq}} \hat{u}(k) \exp(-\imath kx)\, \mathrm{d}k, \tag{4}$$

where $k_{\max} = \pi/\Delta x$ is fixed by the Nyquist criterion. Thus, in the finite difference solution of the Navier–Stokes equation one introduces a filter implicitly if k_{eq} in Equation (4) is different to k. Thus, the performance parameter would be k_{eq}/k as plotted against $(k\Delta x)$. Ideally, for a good numerical scheme this will be equal to a value in the permissible range of the wavenumber—as is the case of the spectral method. This parameter was shown in Figures 15 and 16 of Sengupta and Sengupta [2] and Figure 2 of Nair and Sengupta [7] for various upwind and central schemes. Some of the major schemes are reproduced here in Figure 1 showing only the real part of k_{eq}/k for the upwind schemes. In this figure, the compact difference (CD) schemes that were used by Lele [4] are also shown along with the third- and fifth-order upwind scheme. In the CD schemes, the first derivatives are also treated as unknowns and a set of implicit relations are used to relate the unknowns and their derivatives. Any upwind scheme is equivalent to the next higher-order central difference scheme to which a higher-order numerical dissipation is added implicitly. The capability of a numerical scheme

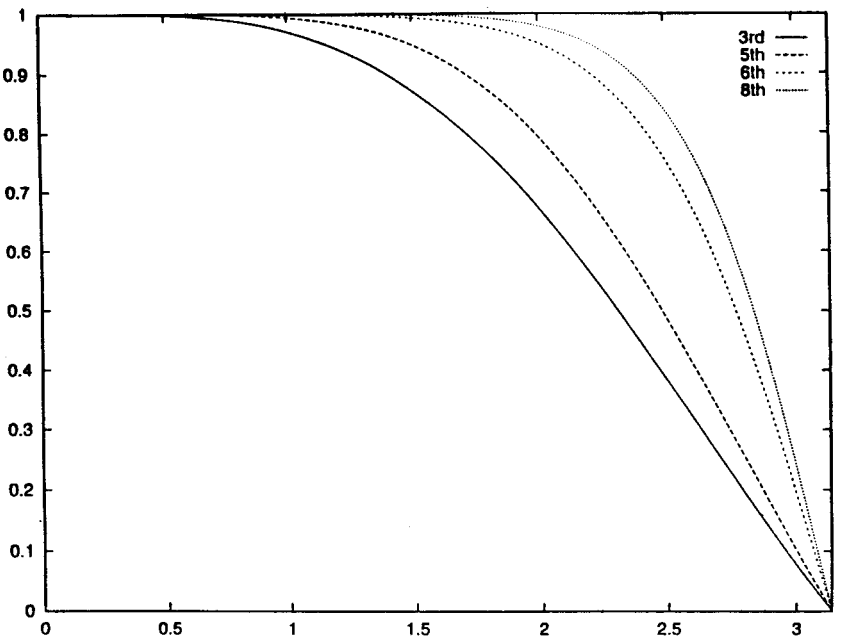

Figure 1. Equivalent non-dimensional phase of third- and fifth-order upwind scheme and sixth- and eighth-order CD scheme versus $k * \Delta x$.

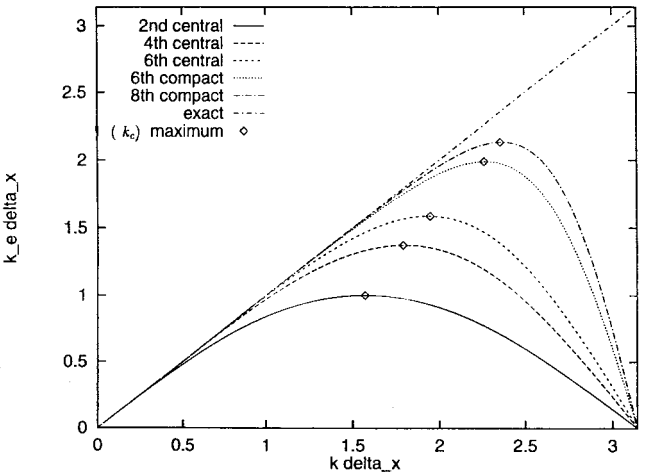

Figure 2. Plot of $k_{eq} * \Delta x$ versus $k * \Delta x$ for the third- and fifth-order upwind and sixth- and eighth-order CD schemes. Also shown is the exact spectral representation.

to simulate high-Reynolds number flows, where a large range of spatio-temporal scales are excited, is directly related to the performance and bandwidth of the filter.

It is often stated (see Schumann [6]) that when the Navier–Stokes equation is solved by a finite difference scheme the filter removes all subgrid scales smaller than the mesh spacing with spatial resolution. This is an exaggeration, as we shall show later, as the discretization also brings in phase error that effectively reduces the maximum wavenumber from its theoretical maximum value of k_{max}. This was shown as Figure 1 in Lele [4], which revealed that the higher wavenumbers are weighted by a smaller value than the actual wavenumber value in Equation (4), as depicted by the folding of k_{eq} to the right of the maximum of the curve and the subgrid scale is determined by the modified maximum wavenumber. Note that the abscissa in that figure is already multiplied by the mesh spacing. In Figure 2 we have shown the correct depiction. In the Figure 15 and 16 of Sengupta and Sengupta [2], the real part represents the phase portrait of Equation (2) and the imaginary part of k_{eq} attenuates the higher wavenumbers. This imaginary part is necessary for numerically stabilizing the solution of the Navier–Stokes equation at a high Reynolds number. Note that some of the spectral DNS procedures add explicitly dissipation terms proportional to the biharmonic terms—which are known as hyperviscosity terms.

Compared with the implicit filters associated with any discretization scheme (except the spectral method) in LES, the filtering of the solution is performed additionally in an explicit manner. The basic numerical methods that are most commonly used are either second- or fourth-order-accurate differencing of the convection terms (see, for example, Moin and Kim [8] for a simulation of channel flow and the general discussion in Ferziger [9]). However, in the choice of filters and eddy viscosity modelling in LES, the implicit filtering associated with the discretization is not considered. Some typical explicit filters used in LES are given in Lele [4] and Spyropoulos and Blaisdell [5]. For a general class of explicit–implicit filter, the transform function is given (as in Spyropoulos and Blaisdell [5])

$$\hat{g}_k = \frac{\sum_{n=0}^{N_e-1} a_n \cos(2\pi k n \Delta x)}{1 + \sum_{m=1}^{N_i} b_m \cos(2\pi k m \Delta x)}, \tag{5}$$

where N_i and N_e are the number of implicit and explicit terms included in the filter and a_n and b_m are the corresponding coefficients. In this reference, a 5-point implicit 7-point explicit filter based on approximating the sharp cut-off filter in a least square sense was found to be the most efficient. However, two points need mentioning: first, one would expect

$$\lim_{k \to 0} \hat{g}_k \to 1 \tag{6}$$

for the filtering to be consistent when one approaches the continuum from the discrete limit. This is not satisfied by this filter (Equation (5)). Second, no filters can violate the Nyquist criteria, i.e.

$$\lim_{k \to k_{max}} \hat{g}_k \to 0. \tag{7}$$

The above-mentioned filter seems to violate this too. If the second condition is violated, it would appear that the filter is able to generate information at the subgrid scale without any additional effort. However, no such problems exist for the filters proposed by Lele [4].

2. RESULTS AND DISCUSSION

Some upwind schemes that have been used by us in the recent past are analysed here. The third-order upwind scheme of Kawamura *et al.* [1] as given by Equation (1) has the following equivalent wavenumber

$$(k_{eq})_{real} = \frac{\sin(k\Delta x)(4 - \cos(k\Delta x))}{3\Delta x},$$
$$(k_{eq})_{imag} = \frac{4 \sin^4(k\Delta x/2)}{\Delta x}, \tag{8}$$

Similarly, for the fifth-order upwind scheme that was used in Nair and Sengupta [7] to simulate flow past elliptic cylinders at an angle of attack at a high Reynolds number, the equivalent wavenumber is given by

$$(k_{eq})_{real} = \frac{\sin(k\Delta x)(2((\cos^2(k\Delta x)) - 6\cos(k\Delta x) + 22))}{60\Delta x},$$
$$(k_{eq})_{imag} = \frac{16 \sin^6(k\Delta x/2)}{15\Delta x}, \tag{9}$$

where $(k_{eq}/k)_{real}$ as given by the first equation of Equations (8) and (9) are shown in Figure 1. Also shown in the figure are the equivalent relations for the sixth- and eighth-order CD schemes proposed by Lele [4] as given by the second and fourth expressions in Table 1 of the cited reference. It appears that the sixth- and eighth-order CD schemes have lesser phase error for all values of k. The actual wavenumbers that are resolved by these schemes are depicted in Figure 2. In this figure, $(k_{eq})_{real} * \Delta x$ is plotted against $k * \Delta x$ and the maximum resolved spatial scale in this paper is defined as the maxima of the curves (k_c)—as indicated in Figure 2. Any wavenumber for which $k_c < k < k_{max}$ is folded back in the wavenumber range $0 < k < k_c$. This is the phase error arising out of discretization. The maxima are not at the Nyquist limit and from Figure 2 one can see that the actual cut-off wavenumber is

$0.43678\pi/\Delta x$ for the third-order upwind scheme, while for the fifth-order scheme $k_c = 0.50478\pi/\Delta x$. Note that the second-order CD schemes in this respect are quite inadequate as $k_{eq} = \sin k\Delta x/\Delta x$ and their use in high-Reynolds number flow would require a very large number of grid points. The numerical dissipation of the third- and fifth-order upwind schemes are given by the second equation of Equations (8) and (9). These dissipation functions are not monotonically increasing functions of $k\Delta x$. The maxima of the third- and fifth-order schemes are at 0.885π and 0.917π respectively. For the sixth- and eighth-order CD scheme the cut-off wavenumber is at $0.633243\pi/\Delta x$ and $0.6797\pi/\Delta x$ respectively. So, in a SubGrid Scale (SGS) LES model one should use an equivalent Δ that should be calculated based on the suggested k_c and that way the used LES model would incorporate the information of the basic numerical methods also. Currently this is not used in LES works.

The successfully computed flows by LES are those for which the large fraction of turbulent energy lies below k_c and is shown in Figure 3. Simulating the dissipation of turbulence energy, the grid spacing must be at least smaller than the length scale corresponding to the peak in the dissipation spectrum (k_2). In the inertial range, the energy $E(k)$ depends only on k and the amount of energy passing down the cascade of scales per unit time, ϵ, such that

$$E(k) = \alpha\epsilon^{2/5}k^{-5/3}, \tag{10}$$

as indicated by the straight line portion of the curve. In the inertial range the motions become homogeneous and isotropic irrespective of the behaviour of motion in the large scales. Thus, in the vicinity of the dissipative peak, the dissipation spectrum is proportional to $k_2^2 E(k_2)$. If η is the Kolmogorov length scale, then it was shown by Leonard [10] that $k_2\eta \cong 0.04$ for the pipe flow experiments reported by Laufer [11], and according to Huang and Leonard [12], a

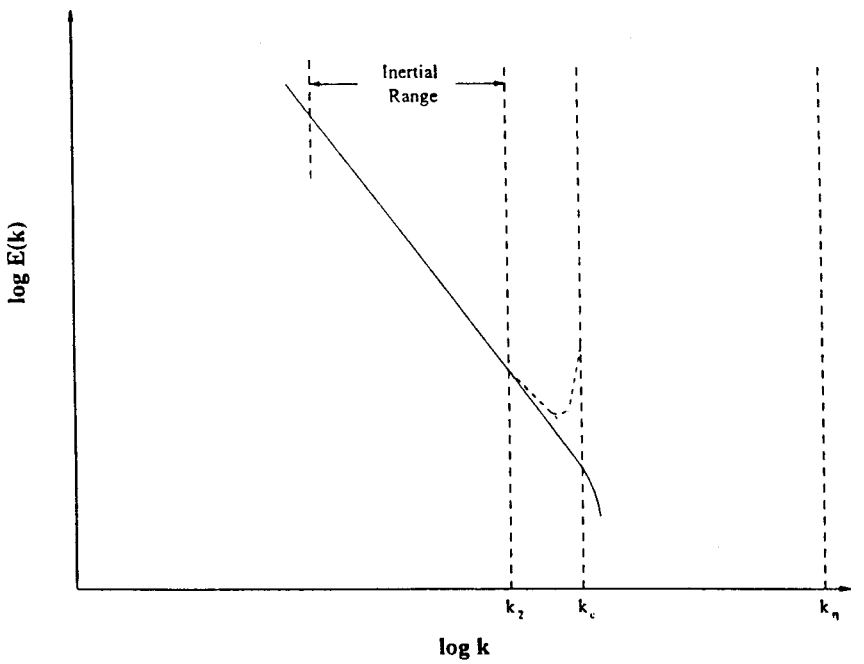

Figure 3. Schematic log plot of turbulent kinetic energy versus the wavenumber. The various important wavenumber limits are shown: k_2 is the dissipation peak, k_c is the cut-off wavenumber and k_η is the Kolmogorov limit. Also note the energy pile-up at k_c in the simulation.

resolution of the fine scales such that $k_c\eta \cong 1$ should be sufficient to emulate the power law decay of homogeneous turbulence. The proper resolution of the scales and energy transfer can be checked by evaluating the energy spectrum of the velocity field

$$E(k) = \frac{1}{2}\int |\hat{u}_k|^2 \, \mathrm{d}k. \tag{11}$$

Now in a simulation with a cut-off wavenumber k_c, if one does not model the subgrid scale associated with various non-linear energy transfers there will be an energy pile-up near k_c—as indicated in Figure 3 owing to aliasing and other non-linear triple interactions. This energy, if not dissipated by an appropriate subgrid scale (SGS) model, will accumulate and modify the slope of the energy spectrum for $k < k_c$ even for short time integration of the Navier–Stokes equation. In well-designed explicit SGS model, the model mimics the mechanism by which the subgrid scale removes energy from the large scale modes by suitably introducing an eddy viscosity. While the phase information is lost in a time integration anyway because of wavenumber truncation, one hopes that the energy spectrum is preserved. The subgrid scale Reynolds stress is usually decomposed into

$$\tau_{ij} = (\overline{\bar{u}_i\bar{u}_j} - \bar{u}_i\bar{u}_j) + (\overline{\bar{u}_i u'_j} + \overline{\bar{u}_j u'_i}) + \overline{u'_i u'_j}, \tag{12}$$

where the first term is due to the resolved scale ($k \leq k_c$), the second term gives the interaction between the resolved and the subgrid scale and is usually responsible for the transfer of energy from the resolved to the subgrid scale and the last term represents the interaction among subgrid scales and causes the energy transfer from the subgrid to the resolved scale. It has been shown by Dubois *et al.* [13] that a successful SGS model must retain the second term even if the last term is not accounted for. However, it should be mentioned that for transitional flows, the last term in Equation (12) is important. This term, which is also known as the backscatter term, cannot be neglected for transitional flows.

The role of the SGS model is to remove the pile-up of energy in the vicinity of k_c. One of the most widely used eddy viscosity models, due to Smagorinsky [14], not only removes the pile-up but is also found to be excessively dissipative at lower wavenumbers. In this model, the eddy viscosity is modelled as

$$\nu_t = (C_s\Delta x)^2|\bar{S}|, \tag{13}$$

where $\bar{S}$ is related to the local deformation tensor. One fixes the coefficient C_s so that the energy spectrum in the inertial subrange is modelled properly. Such a fixed constant (C_s) does not produce desired results and various modifications are proposed. In one of the modifications based on Kraichnan's work on 2-point closure (see Lesieur and Métais [15]), the eddy viscosity is represented as

$$\nu_t(k, k_c) = 0.441 C_k^{-3/2}\left[\frac{E(k_c)}{k_c}\right]^{1/2} \nu_t^*\left(\frac{k}{k_c}\right), \tag{14}$$

where C_k is the Kolmogorov constant and $E(k_c)$ is the kinetic energy at k_c and ν_t^* is the non-dimensional eddy viscosity that reveals a cusp-like behaviour at the cut-off frequency.

The above explicit eddy viscosity model accounts for the cusp resulting from the difference between the *drain* of energy from the resolved scale to the subgrid scale and the *backscatter* which sends the energy in the reverse direction. It has been noted in Lesieur and Métais [15] that the strong backscatter exists in the numerical error inverse energy, which is always present due to the finite word length computation and this needs to be controlled by providing appropriate *feedback* in the basic numerical model.

Let us now take a look at the higher-order upwinding schemes in terms of their performance with respect to LES. These schemes are termed as *pseudo-direct simulation* by Lesieur and Métais [15] because it takes care of the subscale events implicitly by providing numerical dissipation that is a function of wavenumber. The implications are that the introduced imaginary part of k_{eq} in Equations (8) and (9) for the third- and fifth-order upwind schemes respectively introduce numerical diffusion that provides the actual balance of the drain and backscatter across the wavenumber. One can see them plotted as a function of $k\Delta x$ in Figure 4. In this figure, we have plotted $(k_{eq})_{imag}$ of various schemes as a function of k/k_c. In Figure 4(a) and (b) the third- and fifth-order upwind scheme values are plotted while in Figure 4(c) and (d) we have shown the sixth-order CD scheme in conjunction with the fourth- and sixth-order dissipation term. Note that a sixth-order CD scheme in conjunction with fourth- and sixth-order dissipation term constitute the third- and fifth-order upwind schemes respectively. Similarly, in Figure 4(e) and (f), the eighth-order CD scheme in conjunction with the fourth- and sixth-order dissipation term are shown, which are once again third- and fifth-order schemes. It is worthwhile to note that these suggested hybrid schemes of third- and fifth-order upwinding increases the stencil size. To convert the eighth-order CD scheme to a seventh-order upwind scheme one would need to use an eighth-order dissipation term. What is remarkable about these figures is that the behaviour of the numerical dissipation follows the way v_t^* in Equation (14) is expected to vary with k/k_c. It is noted in Lesieur and Métais [15] that v_t^* should be equal to 1 for $k/k_c < 0.3$ and the included numerical dissipation as shown in Figure 4(a)–(f) shows that the third-order scheme very nearly obeys this requirement and the fifth-order scheme satisfies it exactly. Also, it becomes apparent that the CD schemes in conjunction with sixth-order dissipation would be a most appropriate candidate for *pseudo-direct simulation*. The numerical dissipation added does not show a cusp but it does show the required monotonic increase with wavenumber all the way up to k_c.

From the k_c values it would appear that using the sixth- and eighth-order CD scheme would allow one to use them for LES applications at higher Reynolds numbers. However, CD schemes require more memory for the additional unknown derivatives. In Equation (2), with k replaced by k_{eq}, the presence of the imaginary part of k_{eq} changes the amplitude of u to $\hat{u}_k \exp((k_{eq})_{imag}x)$ and thus the different wavenumber component will decay by a different amount at a given distance.

Consider a fluid dynamical system that is excited by white noise, i.e. the system is excited at all frequencies equally. Therefore, we can talk about an equivalent energy amplitude as evaluated as $\exp((k_{eq})_{imag}x)$ at different distances from a given point. In Figure 5(a) and (b) we have shown the normalized energy amplitude as a function of k/k_c at two distances Δx and $2\Delta x$. In these figures we have also shown the corresponding hybrid fifth-order upwind schemes constructed from the CD schemes by adding the sixth-order dissipation term which is the same that is used with the fifth-order upwind scheme given by Equation (9). The figures reveal that the upwinding on these higher-order CD schemes bring their energy amplitude below the level of fifth-order upwind schemes.

The *aliasing errors* appear in numerical computations whenever non-linear terms are computed numerically. For the Navier–Stokes equation this product is furthermore differentiated in the physical space—which is equivalent to multiplying such a product by an equivalent wavenumbers (k_{eq}). As it has been pointed out by Kravchenko and Moin [16] that the aliasing errors are more for spectral method as compared with finite difference methods because the k_{eq} of finite difference methods are lower as compared with the spectral method. In the same way, a lower-order accurate finite difference method will suffer less due to *aliasing error* than a higher-order method. This is a penalty that one has to pay for adopting a higher-order

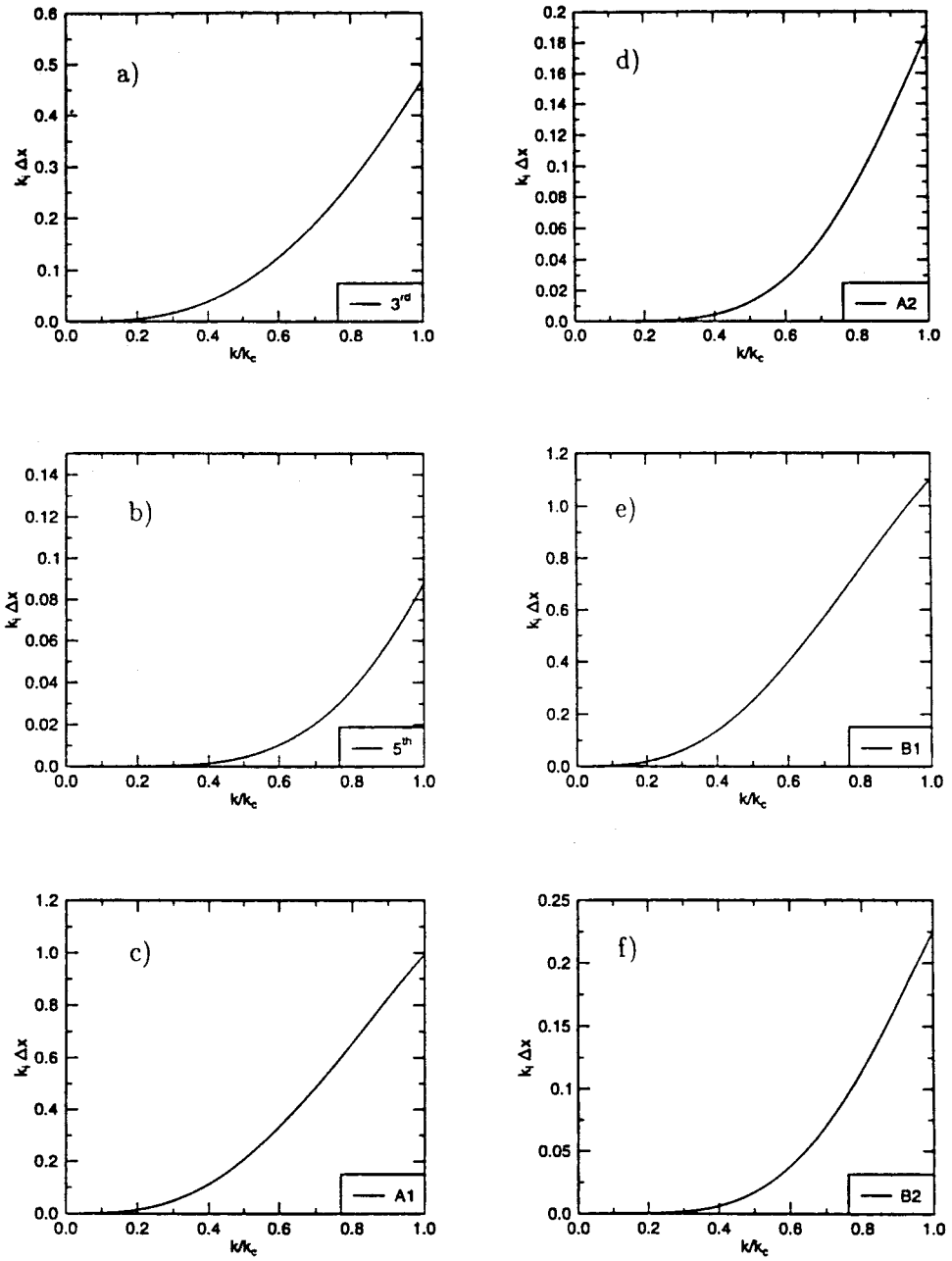

Figure 4. The numerical dissipation of some used and suggested upwind schemes plotted up to their cut-off wavenumbers. (a) Third-order upwind scheme, (b) fifth-order upwind scheme, (c) sixth-order CD scheme with fourth-order dissipation term, (d) sixth-order CD scheme with sixth-order dissipation terms, (e) eighth-order CD scheme with fourth-order dissipation terms, and (f) eighth-order CD scheme with sixth-order dissipation terms.

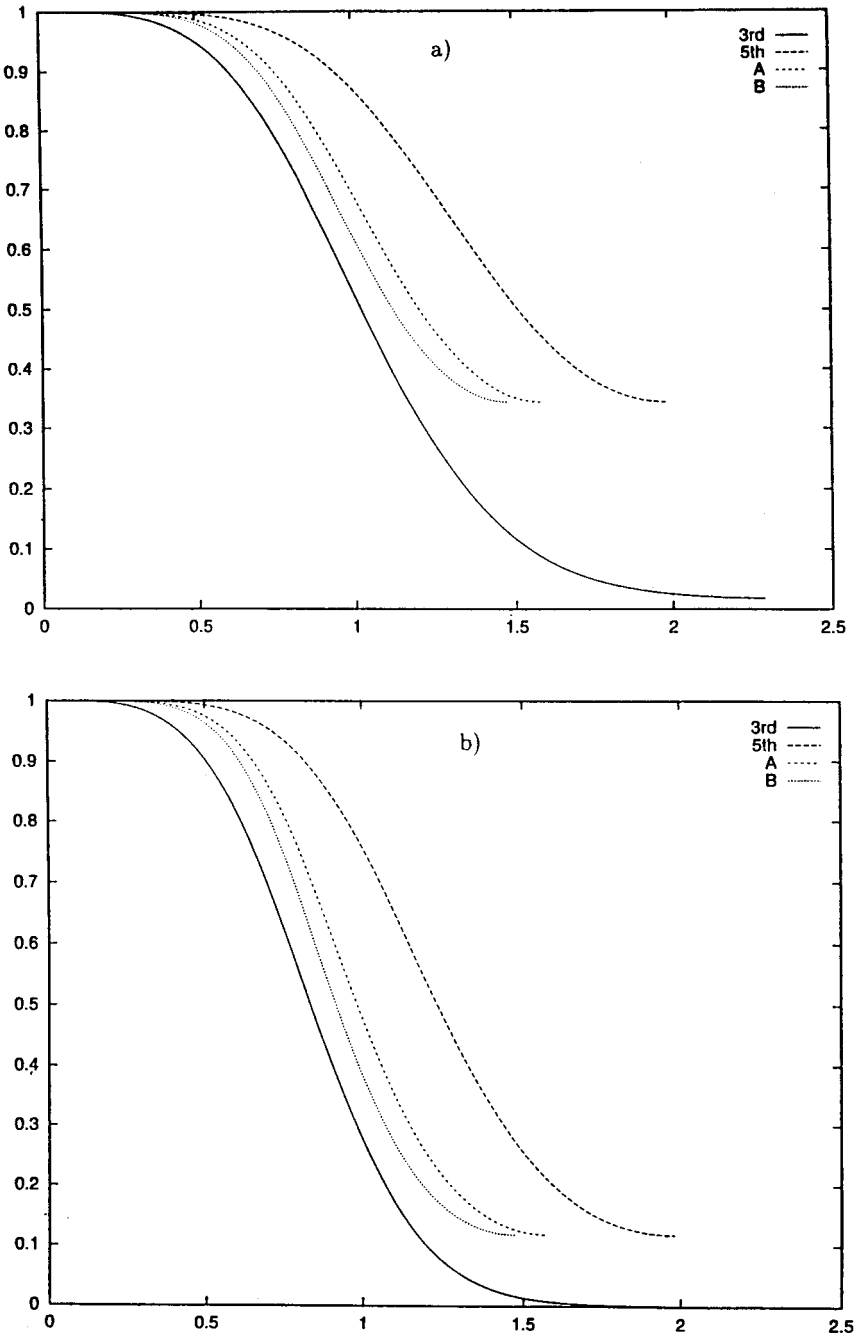

Figure 5. The equivalent energy height versus k/k_c for various upwind schemes. 'A' corresponds to the sixth-order CD with sixth-order dissipation terms and 'B' corresponds to the eighth-order CD with sixth-order dissipation terms. (a) Quantities at Δx and (b) at $2\Delta x$.

method. Since in a finite difference method it is not straightforward to perform *de-aliasing*, this problem can be handled efficiently by adopting skew symmetric differencing of the non-linear term. This has been clearly shown by Kravchenko and Moin [16] who have used it following the original suggestion of Arakawa [17], which was used in meteorological long time calculations for the inviscid vorticity transport equation. Note that the effect of aliasing will be dictated by the portion of the curves, in Figure 5(a) and (b), which are to the right of $k/k_c = 1$ and with the order of the basic numerical methods increasing the aliased part increases. The hybrid CD schemes are somewhat better than the scheme marked 'A' in the figures when compared with the fifth-order scheme. One aspect about the third-order upwind scheme needs emphasising. Although the tail portion of the curve, which can be a source of aliasing, extends beyond $k/k_c = 2.25$ but the energy height of the tail is significantly lower than any of the other methods shown in the figures. Further away from the source, the performance of the third-order scheme is better in terms of the aliasing effect. Thus, the fifth-order upwind scheme is a compromise between a sharp cut-off feature required and the least damping of the resolved scale. There would be marginal improvement in the resolution at the cost of an increase in storage requirement for the CD schemes, but the marked difference between the third- and fifth-order upwind schemes would certainly prompt one to view the fifth order scheme favourably—although based on our own experiences this scheme makes the actual computations very expensive as the time step restriction for an explicit time advancement is severe.

Finally, we would like to point out that for computations that require non-uniform grids, the choice of the upwind method is strongly dependent on the grid itself. As it is shown in Nair *et al.* [18], the third-order scheme when applied in a mapped plane may produce many unintended effects. The biharmonic numerical dissipation of the transformed plane when expressed in the physical plane shows alterations of the basic dynamics. In the above mentioned reference, apart from providing the detailed reasons, some remedies have been provided to avoid the grid dependence problem. In one of the severe criticism of the third-order upwind schemes, Schumann [6] has pointed out that the results using third-order schemes were not shown to be grid-independent. However, if one chooses the type of grids used in Nair *et al.* [18], the results become grid-independent and detailed results are obtained for various geometries in Nair and Sengupta [7] for elliptic cylinders and in Sengupta and Nair ['Unsteady flows past two-dimensional lifting bodies' (under review for *Int. J. Numer. Methods Fluids*, 1999)] for unsteady flows past NACA 0015 aerofoils. In both these references it is shown that the adopted third- and fifth-order upwind schemes are quite capable of capturing the Kelvin–Helmholtz instability in the shear layer transition regime.

3. CONCLUDING REMARKS

In this paper we have evaluated various currently used upwind methods for simulating high-Reynolds number flows. A lot of effort has gone into developing subgrid-scale models for LES that are invariably calibrated with respect to test cases with homogeneous decaying turbulence or some benchmark DNS results. To make the comparisons meaningful, the DNS results are also filtered. Thus, these LES methods have very rarely been tested for inhomogeneous shear flows—the ultimate environment where they are intended to be used. On the other hand, the so-called *pseudo-direct simulation* methods have been used to compute many practical problems but how they perform is not well explained. In this paper their role *vis-à-vis* LES has been compared in resolving various important scales. It is noted that in the process of trying to evolve universal models for the subgrid, no attention has been paid to incorporate

the information of k_c of the basic numerical methods that has been used in the subgrid-scale model. It has been shown that the implicit numerical dissipation of higher-order upwind schemes mimic the required eddy viscosity that models at least the energy spectrum and this is perhaps the reason that the methods are successful in simulating high-Reynolds number flows. We have also pointed out that for the simulation using a higher-order upwind scheme, special attention must be given for the grid used when resolution demands the use of a non-uniform grid. It is seen that the higher-order compact schemes are preferable because of their higher value of k_c. But if they are to be used along with implicit dissipation terms for pseudo-direct simulation then the gains are only marginal over a fifth-order upwind scheme in terms of resolution. Also, they damp the resolved scales significantly as compared with the fifth-order upwind scheme. Since the compact difference schemes also require additional storage space for the unknown derivatives, their use will hardly pay-off. We expect that new classes of explicit subgrid-scale models to be developed in the near future which will use higher-order schemes for the basic numerical methods than the present day second- and fourth-order methods. It is easy to see that a second-order method is just not sufficient—until and unless one uses them with very fine grid resolution. Some work is already in progress in developing explicit subgrid-scale models to be used in conjunction with higher-order dissipationless methods.

REFERENCES

1. T. Kawamura, H. Takami and K. Kuwahara, 'A new higher order upwind scheme for incompressible Navier–Stokes equation', *Fluid Dyn. Res.*, **1**, 145–162 (1985).
2. T.K. Sengupta and R. Sengupta, 'Flow past an impulsively started circular cylinder at high Reynolds number', *Comput. Mech.*, **14**, 298–310 (1994).
3. M.T. Nair and T.K. Sengupta, 'Onset of asymmetry: flow past circular and elliptic cylinders', *Int. J. Numer. Methods Fluids*, **23**, 2765–2780 (1996).
4. S.K. Lele, 'Compact finite difference schemes with spectral-like resolution', *J. Compt. Phys.*, **103**, 16–42 (1992).
5. E.T. Spyrogoulos and G.A. Blaisdell, 'Evaluation of inhomogeneous formulations of the dynamic subgrid-scale model', in M.Y. Hussaini, T.B. Gatski and T.L. Jackson (eds.), *Transition, Turbulence and Combustion*, vol. II, Kluwer Academic, Dordrecht, 1994, pp. 51–60.
6. U. Schumann, 'Direct and large eddy simulation of turbulence', *Von Karman Inst. Lecture Series 1987-06*, 1987, pp. 1–44.
7. M.T. Nair and T.K. Sengupta, 'Unsteady flow past elliptic cylinders', *J. Fluids Struct.*, **11**, 855–895 (1997).
8. P. Moin and J. Kim, 'Numerical investigation of turbulent channel flow', *J. Fluid Mech.*, **118**, 341–377 (1982).
9. J.H. Ferziger, 'Large eddy simulation', in T.B. Gatski, M. Yousuff Hussaini and J.L. Lumley (eds.), *Simulation and Modeling of Turbulent Flows*, Oxford University Press, Oxford, 1996, pp. 109–154.
10. A. Leonard, 'Direct numerical simulation of turbulent flows', in T.B. Gatski, M. Yousuff Hussaini and J.L. Lumley (eds.), *Simulation and Modeling of Turbulent Flows*, Oxford University Press, Oxford, 1996, pp. 79–108.
11. J. Laufer, 'The structure of turbulence in fully developed pipe flow', *NACA 1174*, 1954.
12. M.J. Huang and A. Leonard, 'Power-law decay of homogeneous turbulence at low Reynolds numbers', *Phys. Fluids*, **6**, 3765–3775 (1994).
13. T. Dubois, F. Jauberteau and Y. Zhou, 'Influence of subgrid scale dynamics on resolvable scale statistics in large eddy simulations', *Physica D*, **100**, 390–406 (1997).
14. J. Smagorinsky, 'General circulation experiments with the primitive equations', *Mon. Weather Rev.*, **91**, 99–164 (1963).
15. M. Lesieur and O. Métais, 'New trends in large eddy simulation of turbulence', *Annu. Rev. Fluid Mech.*, **28**, 45–82 (1996).
16. A.G. Kravchenko and P. Moin, 'On the effect of numerical errors in large eddy simulations of turbulent flows', *J. Comput. Phys.*, **131**, 310–322 (1995).
17. A. Arakawa, 'Computational design of long-term numerical integration of the equations of fluid motion: I. Two dimensional incompressible flow', *J. Comp. Phys.*, **1**, 119–143 (1966).
18. M.T. Nair, T.K. Sengupta and U.S. Chauhan, 'Flow past rotating cylinders at high Reynolds numbers using higher order upwind schemes', *Comput. Fluids*, **27**, 47–70 (1998).

